Heliyon 10 (2024) e27216

Contents lists available at ScienceDirect

Heliyon

journal homepage: www.cell.com/heliyon

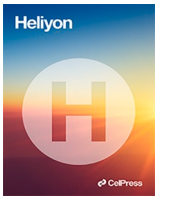

Research article

Bulk anda single-cell transcriptome profiling reveals the molecular characteristics of T cell-mediated tumor killing in pancreatic cancer

Yin-wei Dai [a,1], Ya-ting Pan [b,1], Dan-feng Lin [a], Xiao-hu Chen [c], Xiang Zhou [a,**,1], Wei-ming Wang [d,*,1]

[a] Department of Breast Surgery, The First Affiliated Hospital of Wenzhou Medical University, Wenzhou, China
[b] Department of Gastroenterology, The First Affiliated Hospital of Wenzhou Medical University, Wenzhou, China
[c] Department of Pathology, The First Affiliated Hospital of Wenzhou Medical University, Wenzhou, China
[d] Department of Hepatopancreatobiliary Surgery, The First Affiliated Hospital of Wenzhou Medical University, Wenzhou, China

ARTICLE INFO

Keywords:
T cell-mediated tumor killing
Single-cell sequencing
Immunotherapy
Pancreatic adenocarcinoma
Tumor immune microenvironment

ABSTRACT

Background: Despite the potential of immune checkpoint blockade (ICB) as a promising treatment for Pancreatic adenocarcinoma (PAAD), there is still a need to identify specific subgroups of PAAD patients who may benefit more from ICB. T cell-mediated tumor killing (TTK) is the primary concept behind ICB. We explored subtypes according to genes correlated with the sensitivity to TKK and unraveled their underlying associations for PAAD immunotherapies.
Methods: Genes that control the responsiveness of T cell-induced tumor destruction (GSTTK) were examined in PAAD, focusing on their varying expression levels and association with survival results. Moreover, samples with PAAD were separated into two subsets using unsupervised clustering based on GSTTK. Variability was evident in the tumor immune microenvironment, genetic mutation, and response to immunotherapy among different groups. In the end, we developed TRGscore, an innovative scoring system, and investigated its clinical and predictive significance in determining sensitivity to immunotherapy.
Results: Patients with PAAD were categorized into 2 clusters based on the expression of 52 GSTTKs, which showed varying levels and prognostic relevance, revealing unique TTK patterns. Survival outcome, immune cell infiltration, immunotherapy responses, and functional enrichment are also distinguished among the two clusters. Moreover, we found the CATSPER1 gene promotes the progression of PAAD through experiments. In addition, the TRGscore effectively predicted the responses to chemotherapeutics or immunotherapy in patients with PAAD and overall survival.
Conclusions: TTK exerted a vital influence on the tumor immune environment in PAAD. A greater understanding of TIME characteristics was gained through the evaluation of the variations in TTK modes across different tumor types. It highlights variations in the performance of T cells in PAAD and provides direction for improved treatment approaches.

* Corresponding author. Department of Hepatopancreatobiliary Surgery, The First Affiliated Hospital of Wenzhou Medical University, Wenzhou, Zhejiang, China.
** Corresponding author. Department of Breast Surgery, The First Affiliated Hospital of Wenzhou Medical University, Wenzhou, Zhejiang, China.
E-mail addresses: 601716404@qq.com (Y.-w. Dai), 842059038@qq.com (Y.-t. Pan), 21818316@zju.edu.cn (D.-f. Lin), 594994474@qq.com (X.-h. Chen), zhouxiang36@outlook.com (X. Zhou), wwm_boy2010@163.com (W.-m. Wang).
[1] Contributed equally.

https://doi.org/10.1016/j.heliyon.2024.e27216
Received 25 August 2023; Received in revised form 22 February 2024; Accepted 26 February 2024
Available online 28 February 2024

1. Introduction

Globally, Pancreatic adenocarcinoma (PAAD) is the deadliest gastrointestinal tumor, with a comparable death rate to its incidence [1,2]. With a 5-year survival rate of less than 5%, PAAD is ranked as the third leading cause of cancer-related mortality. Moreover, PAAD is predicted as the second leading cancer-induced mortality in America by 2030. The overall survival (OS) time of patients with PAAD has moderately increased by conventional approaches using radiotherapy and chemotherapy [3]. The past several years have witnessed that immunotherapy and molecular targeted therapy have proved to have favorable effects on subgroups of patients with pancreatic cancer [4]. Promising outcomes have been observed in various cancer types with the use of immune checkpoint blockade （ICB） therapy focusing on CTLA-4 and PD-1. However, PAAD is a low-immunogenic type of malignant tumor with a poor response to ICB [4]. The underlying mechanism is obscure. Nevertheless, certain research suggests that T cell antitumor response is essential for treatments that focus on PD-1/PD-L1 or CTLA-4, implying that traditional cancer immunotherapy may not be effective in treating pancreatic cancer [5]. Through the recognition of tumor-related antigens, T cells, especially antigen-specific cytotoxic T cells, have an ability of detecting and eliminating cancer cells. Immunotherapy relies on T-cell-mediated tumor killing (TTK). Based on TTK sensitivity-related gene expression, Hong et al. constructed subtypes of liver cancer [6]. Their prognostic value has been assessed for immunotherapy. The varying reactions of ICB in individuals with PAAD may be due to unique tumor environments. Consequently, sufficiently understanding the heterogeneity that represents the difference between the mechanisms of immunotherapy treatment and the immune responses of patients with PAAD is of great interest. Therefore, TTK-related features in PAAD and their value in clinical outcome and response to immunotherapy remain to be explored.

Zhang et al. constructed an immune-Related risk model [7]. Moreover, Xu et al. identified two novel pancreatic cancer $CD8^+$ T cell-related phenotypes and developed a $CD8^+$ T cell-related risk model [8]. However, these studies were not validated and analyzed based on the single-cell sequencing level. Therefore, the exploration of the heterogeneity of tumor immune microenvironment (TME) based on model is not adequate.

Pan et al. conducted a CRISPR-Cas9 screen at the genome scale. It was discovered that deactivating several genes associated with TTK resistance could make tumor cells more susceptible to T cell-induced cell death and enhance the effectiveness of immunotherapy [9]. Ru et al. discovered that CD47 and PTPN2 control tumor susceptibility to T cell-induced cell death (known as GSTTK) and immunotherapy through the analysis of genomic profiling data and high-throughput screening [10].

This study utilized a group of GSTTK for the initial time to detect the diversity of immune cell infiltration characteristics and immunophenotypes in PAAD patients using scRNA-seq and multi-omics data. Lastly, this study used a new scoring system, named TRGscore, according to the expression profiles of GSTTK. We illustrate that TRGscore could serve as an indicator of survival outcome, TME, and immune response to immunotherapy in PAAD. Our analysis revealed an association between survival outcome, tumor microenvironment (TME), and the effectiveness of immunotherapy in PAAD. The TRGscore were further explored at single cell levels in order to illustrate the underlying heterogeneity of immune landscape between TRGscore-high and -low group. Overall, for more precise and individualized medicine, TRGscore offers a promising tool for development of new treatment strategies.

2. Materials & methods

2.1. Raw data preprocessing

Clinical data and transcriptional information were acquired from the Genotype Tissue Expression Project (GTEx) and The Cancer Genome Atlas (TCGA) databases [11], respectively. Moreover, specimens with a survival time of <1 month were eliminated. The ICGC PACA-CA cohort [12] and *meta*-PAAD cohort (GSE21501, GSE57495, and GSE71729) [13] were utilized to validate the repeatability of our concluded results. The ComBat algorithm from the 'sva' package in R helps reduce the batch effects caused by non-biological technical biases in each dataset. A total of 641 genes were obtained from the Tumor-immune system interactions and drug bank database (http://cis.hku.hk/TISIDB/) [10], known as GSTTK. We screened differentially expressed genes (DEGs) by comparing gene transcription profiles from the GTEx and TCGA databases using the R package "limma." After selecting the overlap with GSTTK, 328 genes related to GSTTK were curated. The hub genes found by GSTTK to be associated with OS in PAAD were selected using univariate Cox regression analysis with the survival package in R, requiring a p-value of less than 0.05 and a hazard ratio (HR) greater than 1. scRNA-seq data were derived from five samples (GSM4730260, GSM4730261, GSM4730262, GSM4730263, and GSM4730264) in GEO: GSE156405.

2.2. Consensus clustering

The TCGA cohort's cluster count was determined using hub genes through a consensus clustering algorithm and subsequently validated in the ICGC PACA-CA and *meta*-PAAD cohorts. Moreover, the package ConsensusClusterPlus was utilized to run and repeat this process 1000 times in R.

2.3. Evaluation of immune cell infiltration in the TME

The proportions of immune cells were explored utilizing the CIBERSORT [14] and MCPcounter [15] algorithms, and their immune function was estimated in the TME. An ssGSEA was conducted to uncover the proportional distribution of immune cell infiltration

levels in the TME [16]. Describing the seven steps in the cancer immunity cycle revealed the anticancer immune response in a previous article [17]. Immune and stromal scores were evaluated according to the "Estimate" package in R [18].

2.4. Mutation analysis

Our study evaluated the TMB scores for each sample with PAAD in the clusters using mutation annotations from the TCGA database developed by the "maftools" R package.

2.5. Functional and pathway enrichment analyses

In addition to analyzing the Hallmark gene sets, we obtained a collection of gene sets that represent distinct biological processes, as created by Mariathasan and colleagues [19]. The list of factors includes antigen processing machinery, angiogenesis, CD8 T effectors, base excision repair, DNA replication, DNA damage repair 1 and 2, Fanconi anemia, epithelial-mesenchymal transition (EMT), immune checkpoint, homologous recombination etc. (Supplementary Table 4) [19–21]. Additionally, we compared the activity of the above-mentioned pathway signatures between distinct GSTTK-related clusters.

Gene sets for inhibitory immune checkpoints and immunomodulators, containing chemokines, receptor molecules, major histocompatibility complex molecules and immunostimulant molecules were acquired [22–24] (Supplementary Table 4). The Wilcoxon rank sum test was conducted to assess the gene expression levels in different subtypes of PAAD.

A prevalent approach, T cell inflammatory signature (TIS), was conducted to evaluate the immunotherapeutic response between different clusters. SsGSEA algorithm scored TIS containing 18 inflammatory genes, which indicated a better response to PD-1 blockade based on a higher score [25].

2.6. Construction of GSTTK-related gene score

We acquired DEGs in TCGA-PAAD classified by the two GSTTK patterns to construct a scoring algorithm according to GSTTK-related genes. Next, the TCGA-PAAD dataset was analyzed with univariate Cox regression for correlations between DEGs and OS. We ran principal component analysis (PCA) according to prognostic GSTTK-related DEGs, and then developed the TRGscore using a method referred to PRGScore [26,27] to evaluate the quantification of the GSTTK state at the transcriptomic level. TRGscore is defined as:

$$\mathrm{TRGscore} = (\mathrm{PC1} + \mathrm{PC2}) \ * \sum \mathrm{expi}$$

where PC1 and PC2 are the first two principal components stemming from PCA, and expi is the expression level of GSTTK-related genes. An individual cell's TRGscore were calculated by averaging the expression levels of GSTTK-related genes in the scRNA-seq dataset. We analyzed TRGscore using the R package "Seurat" and its function "AddModuleScore" [28].

2.7. Drug susceptibility analysis

This study utilized the pRRophetic R package to evaluate the sensitivity for universally chemotherapeutic drugs according to their semi-inhibitory concentration (IC50) values.

2.8. The Prediction of immunotherapy response

An immunophenotypic score (IPS) was obtained from the Cancer Immunome Atlas for samples in the TCGA(https://tcia.at/). By examining the TIDE score (http://tide.dfci.harvard.edu/), we forecasted the effectiveness of TRGscore in immunotherapy. Moreover, utilizing the IMvigor210CoreBiologies R package, the transcriptome data, survival data, and immunotherapy effects of the IMvigor210 cohort were curated [19]. We utilized IMvigor210 immunotherapy cohorts to predict immunotherapy response according to TRGscore. We calculated the TRGscore of every patient in IMvigor210 cohorts to explore the influence of the TRGscore on immunotherapy. Patients were divided into two categories: partial remission (PR)/complete remission (CR) and progressive disease (PD)/stable disease (SD) cohorts.

2.9. Identification of significant genes

DEGs were screened by comparing among clusters in TCGA-PAAD, ICGC PACA-CA, and *meta*-PAAD cohorts via the package limma in R ($P < 0.05$) and selecting the top 700 genes according to the avg_log2FC. Significant genes were obtained by intersecting three cohort DEGs.

2.10. Cell lines and reagents

The Panc-1, PATU-8988 and HPNE cells were obtained from the Chinese Academy of Sciences Cell Bank (Shanghai, China). They were grown in Dulbecco's Modified Eagle Medium with 10% fetal bovine serum from Gibco, Thermo Fisher Scientific in Waltham, MA,

USA. The cells were kept at a temperature of 37 °C with a carbon dioxide concentration of 5%.

2.11. Extraction of RNA and quantitative real-time polymerase chain reaction (PCR) analysis

Tumor cells were conducted to extract total RNA with TRIzol Reagent (Invitrogen, Carlsbad, CA, USA) according to the manufacturer's guidelines. A 7500 Real-Time PCR Detection System was applied to perform quantitative real-time PCR (qRT-PCR). The analysis of the results was conducted using the $2-\Delta Ct$ technique, with GAPDH serving as the reference control. The gene primers included CATSPER1 with the forward sequence 5′-GAGTTCCAAGACTTCCACGACCAAG-3′ and reverse sequence 5′-TGAGAGGGAGCCAGACCAAAGC-3′, as well as GAPDH with the forward sequence 5′-GGAGCGAGATCCCTCCAAAAT-3′ and reverse sequence 5′-GGCTGTTGTCATACTTCTCATGG-3′.

2.12. Cell proliferation assay

Cell viability assays are performed in vitro using a Cell Counting Kit-8 at 0 h, 24 h, and 48 h time points, measuring at 450 nm. Additionally, colony formation assays are used to investigate the impact of CATSPER1 on the proliferation of pancreatic cancer cells [29], as suggested by previous studies.

2.13. Transfection

siRNAs targeting CATSPER1 and non-targeting scrambled negative control (NC) siRNAs were acquired from GenePharma in Suzhou, China. The cells were seeded and cultured in six-well plates with a density of 2×10^5/well overnight. Then, cells were transfected with siRNA or NC using Lipo3000 Transfection Reagent (GLPBIO, USA) (GK20006) [30]. Small interfering RNA (si-RNA) delivered to cells by Lipo3000 (GLPBIO, USA) decreased the expression of CATSPER1. Cells were collected for subsequent tests after a 24-h cultivation period. The efficiency of the transfections was investigated after 24h using RT-PCR. In this article, the siRNA sequences targeting CATSPER1 were si-CATSPER1-1 (forward: 5′-GCGUGGGAUAUCUGACUAUTT-3′, reverse: 5′-AUAGUCAGAUAUCCCACGCTT-3′) and si-CATSPER1-2 (forward: 5′-GCCUCUCGUACUUCUUUGATT-3′, reverse: 5′-UCAAAGAAGUACGAGAGGCTT3′).

2.14. Immunohistochemical staining

Between January 2015 and December 2018, 65 samples of human PAAD tissues and 78 samples of human PAAD para-tissues were collected from patients who had received cancer resection surgery at the First Affiliated Hospital of Wenzhou University. The Ethics Committee of the First Affiliated Hospital of Wenzhou Medical University [ys 2022(043)] reviewed and granted approval for this study.

Afterward, the tissues were fixed in formalin, encased in paraffin wax, and cut into sections that were 4 μm thick. CATSPER1 primary antibodies (1:200, ab215191, affinity) were applied to the sections and incubated overnight at 4 °C, followed by secondary biotinylated goat anti-rabbit antibodies.

The staining intensity was estimated as follows: 0, none; 1, weak; 2, medium; and 3, strong. The Immunoreactivity Score (IRS) was determined by multiplying two subscores, resulting in a range of 0–12. CATSPER1 was classified as having low expression if IRS was less than 6, and as having high expression if IRS was 6 or greater.

2.15. scRNA data processing

The GSE156405 single-cell sequencing data was procured from the GEO database. Next, we implemented a standardized analysis procedure using the R package "Seurat." Finally, we orderly utilized "NormalizeData," "RunPCA," "FindNeighbors," and "FindClusters" which are based on the k-nearest neighbor classification (KNN) algorithm to process the data [31].

2.16. Cell type classification

Cell types in the sample datasets were identified by annotating each cell type using established marker genes to determine average expression and expression ratio.

2.17. Enrichment score

The hallmark genesetss were then compared between different TRGscore-subgroups using GSEA.

2.18. Cell–cell communication analysis for TRGscore-related subtypes

The CellChat application can uncover intercellular communication networks between different clusters of cells in scRNA-seq data [32]. Initially, we employed CellChat to examine the primary signaling interactions within TRGscore subgroups by utilizing CellChatDB for human data. Additionally, we utilized the netVisual_circle function to display the intensity or quantity of cell-to-cell communication networks originating from the target cell cluster toward various cell clusters within TRGscore-subgroups.

Ultimately, significant differences in ligand-receptor interactions between the two TRGscore-subgroups are delineated by the bubble plots.

2.19. SCENIC analysis

The enrichment of transcriptome factors in cell subtypes was analyzed by running the R package [33]. Raw UMI counts were used as inputs for each sample in SCENIC. All genes whose expression was detected in at least 0.1% of cells in excess 3 times 0.01 were retained. Following this, the AUCell analysis was conducted to evaluate the performance of each regulon in individual cells, by combining expression rank assessment for all genes within a regulon, using the area under the recovery curve.

2.20. Statistical analysis

Differences between the two clusters were identified with the Wilcoxon test. A *t*-test was utilized to compare continuous variables that followed a normal distribution among two distinct groups. The Pearson correlation was performed to evaluate the correlations between variables. Survival curves for the subsets in each cohort were delineated using the Kaplan-Meier technique, with significant differences identified through the log-rank test. Statistically significant results are typically indicated by p-values less than 0.05. R, version 4.1.0 was utilized for all statistical computations.

3. Results

3.1. Data processing

A schematic of the study design is exhibited in Fig. 1.

3.2. Hub gene screening

The data of TCGA and GTEx were derived from UCSC Xena Database. RNAseq data and clinical data from 177 pancreatic cancer samples and 171 normal samples were procured for further analyses after classification and screening. Through differential analysis, we discovered that 166 GSTTK genes were increased and 162 GSTTK genes were decreased, overlapping with the GSTTK genes (FDR <0.05, $|\text{fold change}| > 0.5$) as shown in Supplementary Table 1. These genes were further conducted by univariate Cox regression with a p-value of <0.05 and HR of >1, ultimately named hub genes (Supplementary Table 2).

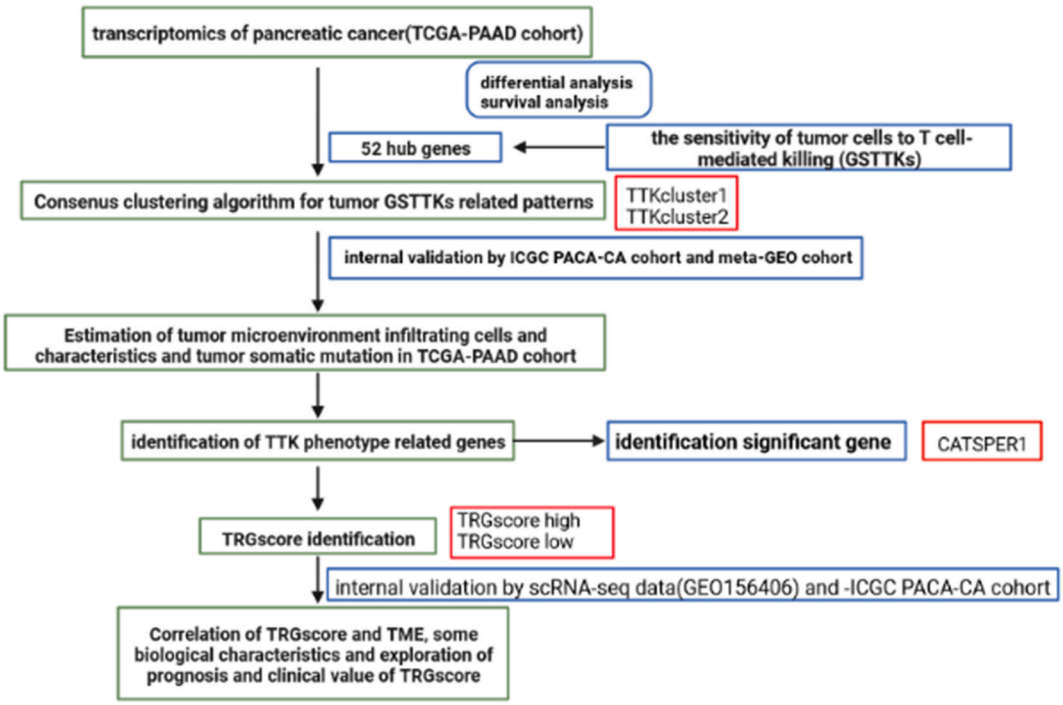

Fig. 1. Overview of the process flow. GSTTK: genes regulating the sensitivity of T cell-mediated tumor killing, TTK: T cell-mediated tumor killing.

3.3. Various TTKS-related patterns discovered through unsupervised learning

Unsupervised clustering in the TCGA cohort revealed the presence of two separate TTK clusters based on 52 hub genes, as shown in Fig. 2A. The Kaplan–Meier analysis elucidated the cases in Cluster 2 associated with poorer outcomes ($p = 0.017$) (Fig. 2B). The results mentioned above can be replicated in the ICGC PAAC-CA cohort ($p < 0.001$) and *meta*-PAAD ($p < 0.001$) cohort to demonstrate the classifier's resilience (Fig. 2C–F).

3.4. TME immune cell infiltration in unique TTKS-related patterns

Cluster 1 associated with TTKS may indicate improved survival rates and is strongly linked to elevated estimate, stromal, and immune scores as determined by the ESTIMATE algorithm (Fig. 2G). The MCPcounter algorithm was used to assess the proportion of immune cells infiltrating the TME, aiming to identify specific differences between TME and TTKS-related patterns. The radar displayed the prominent TTKS-related groupings (Fig. 3A). Cluster 1 showed high levels of immune cell infiltration in the TME, including increased numbers of B cells, T cells, cytotoxic lymphocytes, endothelial cells, CD8 T cells, monocytic cells, NK cells, and myeloid dendritic cells (DCs). The ssGSEA method, which considered the infiltration of immune cells, also reveals similar findings (Fig. 3D). Some research has suggested that the numerous $CD8^+$ T cells play a role in the responsive reaction to immunotherapy. The TME exploration of TTKS-related patterns among the ICGC PAAC-CA and *meta*-PAAD cohorts could further highlight the stability of the classifier (Fig. 3B and C).

Additionally, our results illustrated a more abundant chemokine infiltration in Cluster 1, involving CCL5, CXCR4, CXCL6, CXCL10, CXCL12, and CXCL14 (Fig. 4A, upper part), which attract CD8 + T cells and DCs. The interleukin infiltration level and other cytokines in Cluster 1 were also higher (Fig. 4A, middle and lower parts). Interestingly, the expression of major histocompatibility complexes (MHC) was more down-regulated in Cluster 2 (Fig. 4A, down). J M Kim et al.confirmed that the MHC downregulation on cancer cells is related to immune escape [34]. Of note, the profiles of immune marker genes in the two patterns were further probed. Results on

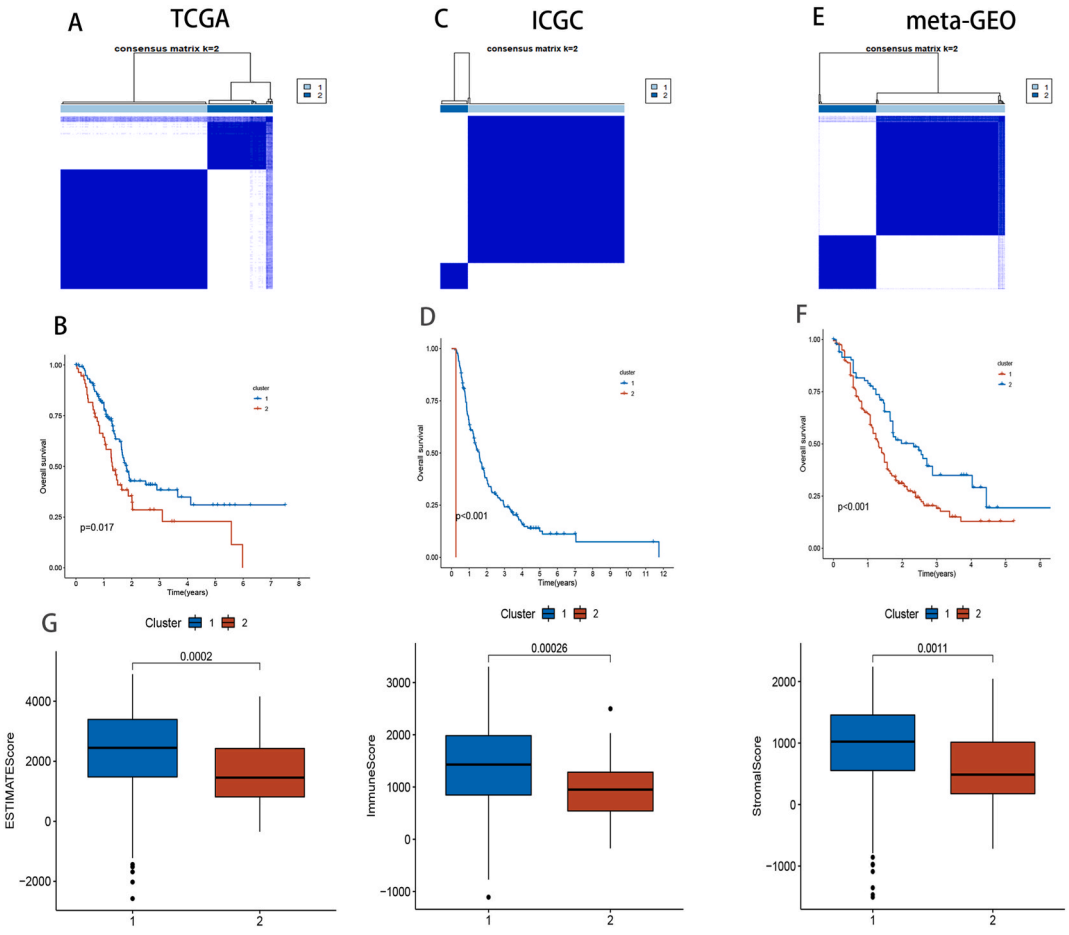

Fig. 2. Unsupervised consensus clustering method (K-means) was used to generate consensus matrices for patients in the TCGA(A), ICGC(B), and *meta*-GEO(C) cohorts. Survival analysis of the different clusters in the TCGA (D) and ICGC (E) cohorts and *meta*-GEO (F). Assessment of the TME in the two TTK associated designs(G).

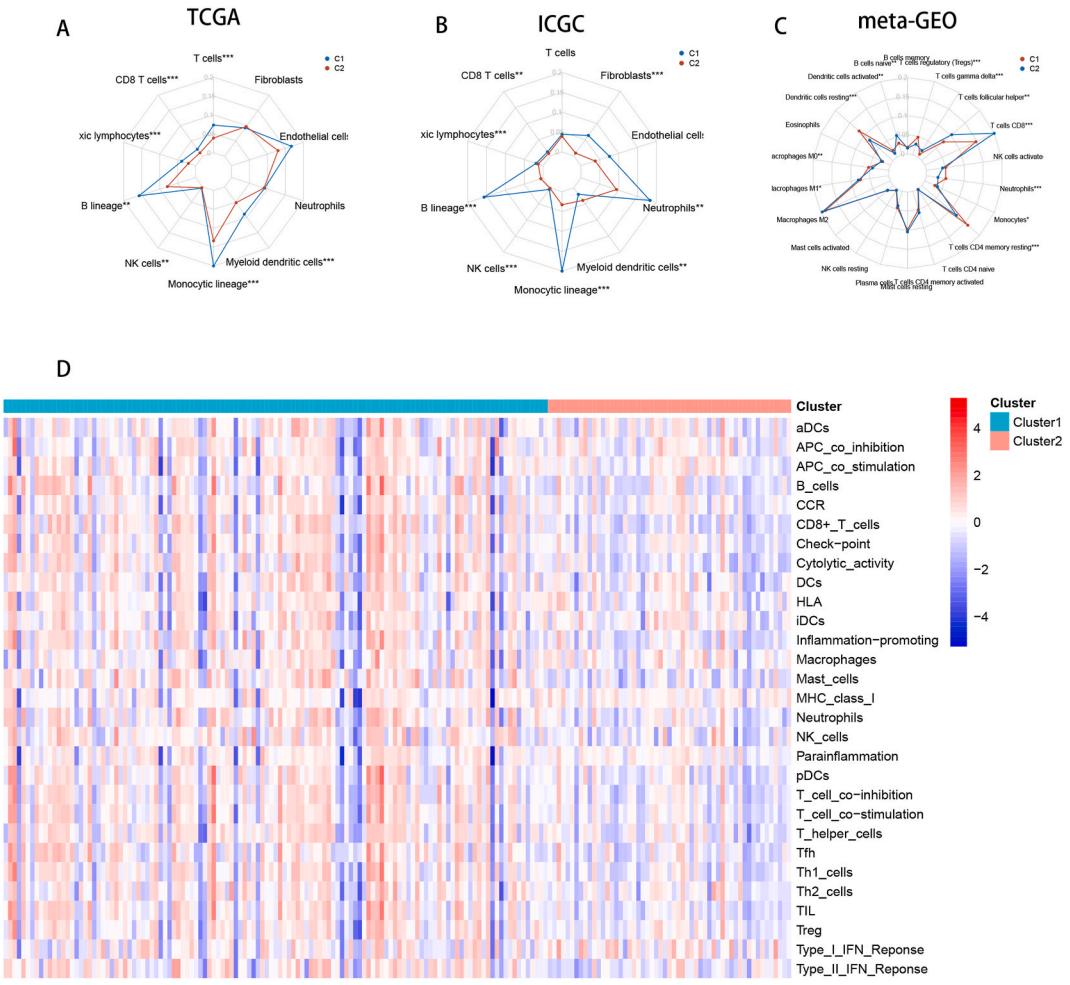

Fig. 3. Variability in levels of immune cell infiltration was observed in two clusters analyzed in TCGA(A) and ICGC(B) cohorts using MCPcounter, and in the *meta*-GEO(C) cohort using CIBERSORT. Visualization of immune reactions within the TTK-associated clusters using ssGSEA(D) heatmap.

patients in Cluster 2, who had high amounts of the macrophage marker gene CD68, suggested that macrophages may exert a profound influence on tumor development (Supplementary Fig. 1). On the other hand, individuals in Group 1 exhibited more positive outcomes due in part to increased expression of genes associated with T cell exhaustion like HAVCR2 and PDCD1, markers for activated T cells like CD3E, ZAP70, ITK, and IL2RB, and indicators of cytolytic activity such as GZMA and PRF1 (see Supplementary Fig. 1).

Some studies indicated that antibodies targeting PD-1 or its ligand, PD-L1, can trigger exhausted CD8 T cells within tumors to boost greater growth and resurge immune response against cancer cells [35–38]. Furthermore, the increased presence of immune checkpoint proteins in Cluster 1, including PD-L1, CTLA4, PDCD1LG2, TNFSF14, TIGIT, etc. (Fig. 4B), provides additional evidence that patients in Cluster 1 may benefit more from immunotherapy compared to those in Cluster 2. Additionally, we analyzed the differences in immune-related gene set scores between the two subtypes. Higher immune checkpoint, angiogenesis, and CD8 T-effector signature gene sets were found in Cluster 1 (Fig. 4C) [39]. Conversely, Cluster 2 possesses more tremendous DNA damage repair ability (Fig. 4D). Comparing the enrichment scores of 10 pathways associated with carcinogens in the two groups was done using the signature published in Ref. [40] (Supplementary Table 4). In Cluster 1, signal pathways like RAS and NOTCH had higher scores (all $P < 0.05$), while Cluster 2 showed a prevalence of PI3K and Wnt pathways (all $P < 0.05$, Fig. 4E).

These results proved repetitive in ICGC, merge-GEO cohort (Supplementary Figs. 2 and 3). Fig. 5A shows that TTK-related Cluster 1 was markedly activated in stromal and immunity pathways. However, TTK-related Cluster 2 was deeply correlated with carcinogenic and glycolysis-associated pathways. Aggravated glycolysis pathways can facilitate tumor proliferation and impair antitumor immunity [41]. Taken together, Cluster 1 is characterized as “hot tumors”, due to being more abundant with immune infiltration levels. In contrast, Cluster 2 features “cold tumors.” Clinical efficacy among distinct clusters was further explored using TIS methods to elucidate immunotherapy. Expectedly, a higher TIS score in Cluster 1 indicated immune activation and a favorable immunotherapy response ($P = 0.00013$) (Fig. 5B).

Tumor genomic mutation associated with antitumor immunity has been elaborated [42]. Hence, we also noticed a conspicuously more frequent mutation in the TTK-related Cluster 1 vs. the TTK-related Cluster 2 ($P = 0.00038$) (Fig. 5C). Yago Pico de Coaña et al.

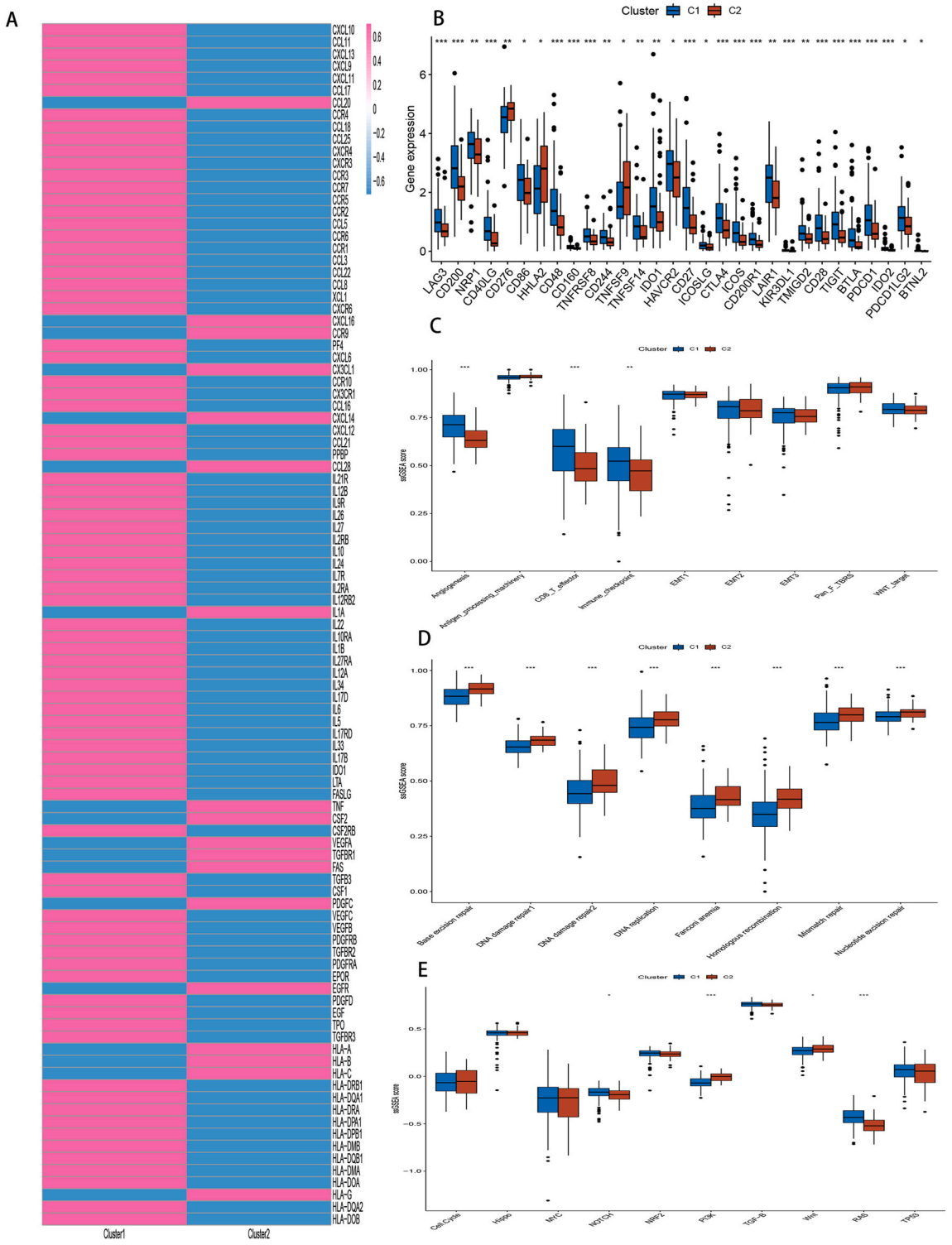

Fig. 4. Both patterns exhibit expression of chemokines, receptors, MHC molecules(A), and immune checkpoint-related genes(B). In the TCGA-PAAD cohort, boxplots showed distinct TTK-related patterns based on TME-related signatures (C, D).The score comparison of 10 pivotal cancerogenic signaling pathways amongs two TTK related patterns were illustrated(E). *P < 0.05, **P < 0.01, ***P < 0.001, ****P < 0.0001.

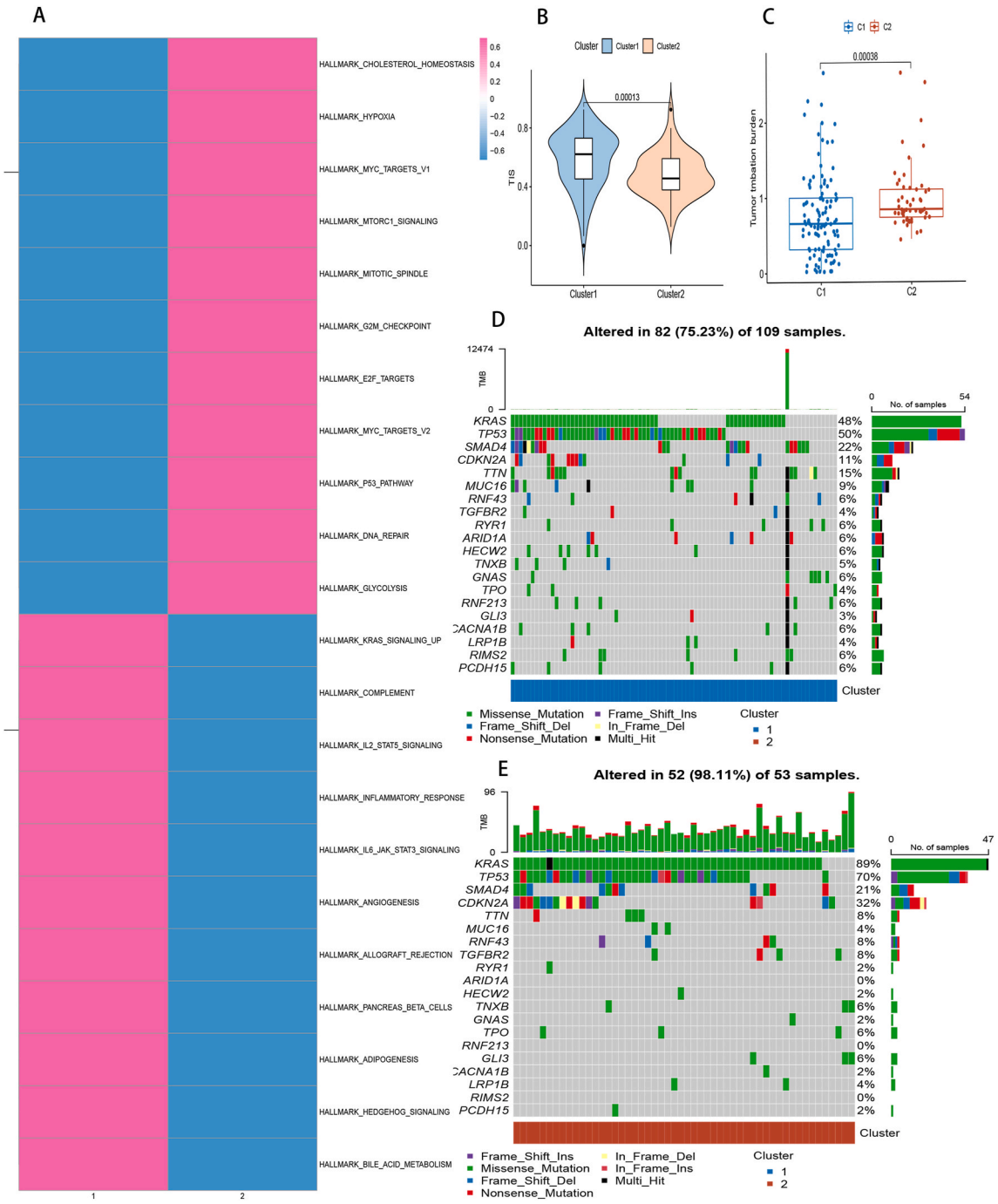

Fig. 5. Biological pathways activation status was compared between two patterns using ssGSEA enrichment analysis (Kruskal-Wallis test, $P < 0.05$), where red indicates activation and blue indicates inhibition(A). Correlation between the TMB and the two TTK related patterns(B). Significantly mutated genes in the patients with PAAD in the different patterns. There were significant mutations in the genes of the PAAD patients according to the different patterns. Genes that have been mutated (rows, top 20) are ranked by mutation rate. The right panel displays the percentage of mutations, while the top panel shows the total number of mutations. Mutation types are indicated by color coding (C, D).

demonstrated that a large amount of tumors can lead to immune system suppression, resulting in resistance to PD-1/PD-L1 inhibitors in cancer [43]. Fig. 5D and E revealed that mutation of most genes was more significantly prominent in the TTK-related Cluster 2, such as KRAS, TP53, SMAD4, and CDKD2A. Events initiated by KRAS mutations, such as cellular autophagy, changes in metabolism, and continuous activation of the yes-associated protein pathway, combine to result in immune evasion [44]. Mut-TP53 can accelerate tumor progression and metastasis by triggering immunosuppressive properties of the PAAD [45,46]. The TGF-β pathway mediated by

SMAD4 suppresses the immune system response, assisting tumor cells in evading immune reactions [47].

3.5. Identifying DEGs between clusters among datasets

The intersections of the top upregulated genes in the three databases revealed four genes (CATSPER1, TNFRSF12A, S100A2, and S100A6) that may contribute to tumor invasiveness to determine whether Cluster 2 tumors possess unique transcriptome programs that might facilitate their deteriorated phenotype (Fig. 6A) (Supplementary Table 3). However, the roles of CATSPER1 and TNFRSF12A in pancreatic cancer have not been experimentally demonstrated.

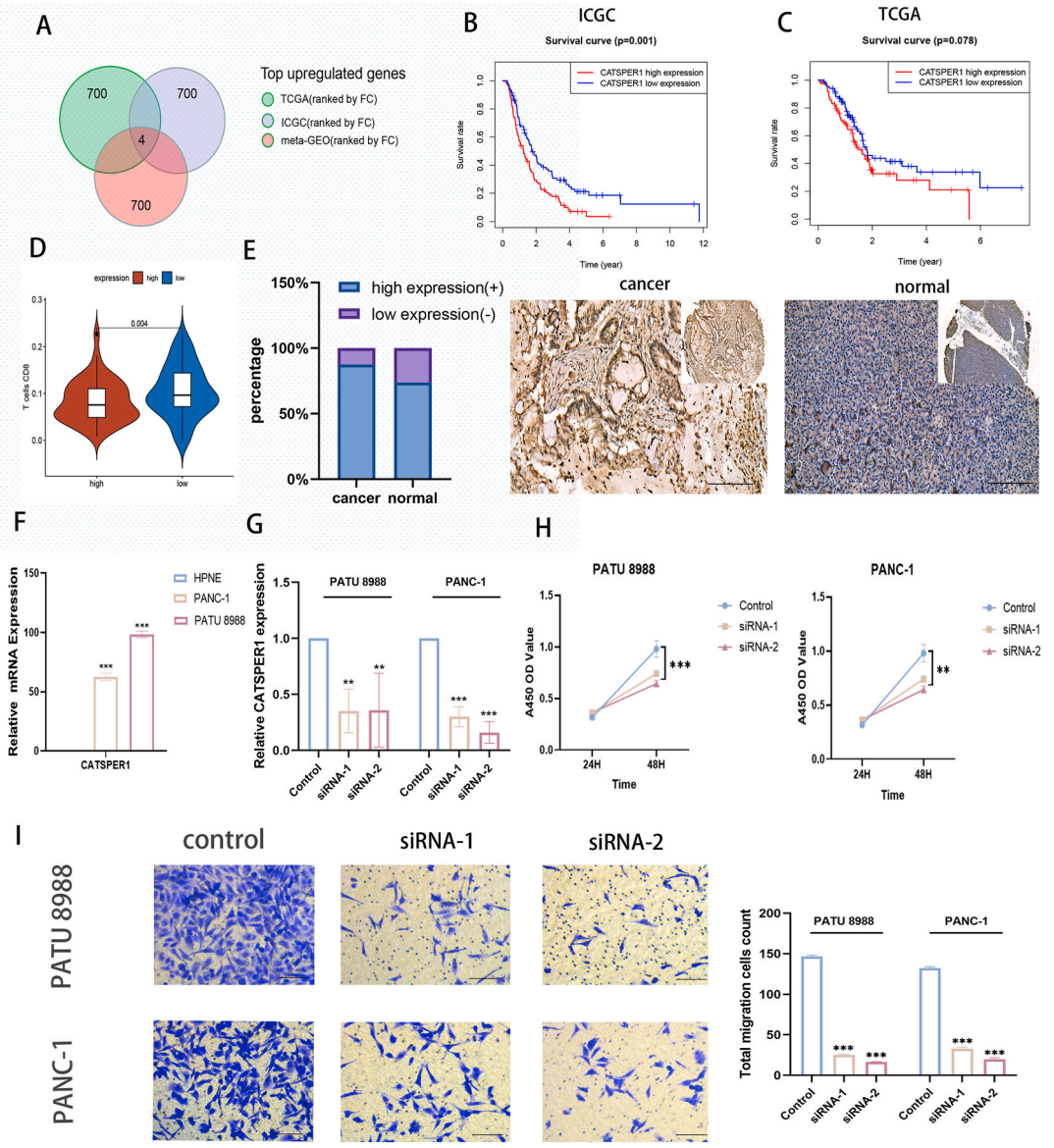

Fig. 6. Verification of hub gene.Venn diagram showing 4 Intersection genes as the candidate (A). CATSPER1's median expression level served as the threshold for overall survival in both ICGC (B) and TCGA cohort (C). The difference of level of $CD8^+$ T cells between CATSPER1 -high and -low groups (D). CATSPER1 was immunohistochemically stained in PAAD and normal tissues using samples from the First Affiliated Hospital of Wenzhou University cohort. Bar = 50 μm (E). PCR analysis revealed the associated CATSPER1 expression in Panc-1 and PATU-8988 cell lines when compared to normal cell lines (F). PCR testing revealed the impact of reducing CATSPER1 in Panc-1 and PATU-8988 cell lines(G). Cell proliferation was assessed using the CCK-8 assay following the knockdown of CATSPER1 in Panc-1 and PATU-8988 cell lines (H). Inhibition of CATSPER1 using the Transwell invasion assay resulted in decreased cellular invasion of Panc-1 and PATU-8988. Visual depiction showing the quantity of invasive Panc-1 and PATU-8988 cells in each microscopic area. Bar = 100 μm (I). Contrast in the relative levels of CATSPER1 expression in PAAD and healthy tissues. *$p < 0.05$,**$p < 0.01$,***$p < 0.001$.

3.6. Cellular experiment integrated biological information unravel the role of CATSPER1 on PAAD

The PCR test showed increased levels of CATSPER1 in Panc-1 and PATU-8988 cells, as depicted in Fig. 6F. Unfortunately, the expression of TNFRSF12A has no significant difference between tumor and normal cells. Additionally, CATSPER1 immunohistochemical pictures were obtained from the cohort at the First Affiliated Hospital of Wenzhou University (Fig. 6E). The result has illustrated higher expressions of CATSPER1 genes in pancreatic carcinoma ($p = 0.0409$). CATSPER1 emerged as the key gene associated with prognosis in the ICGC PACA-CA cohort ($P = 0.001$) and TCGA-PAAD cohort ($P = 0.078$) based on survival analysis findings from Fig. 6B and C. The immunological study revealed that increased CATSPER1 expression was associated with decreased $CD8^+$ T cell infiltration levels (chi-square, $P = 0.004$) (Fig. 6D). Consistently, highly expressed CATSPER1 suggested low enrichment scores of several immune-related pathways and high enrichment scores of the oncogenic pathway (Supplementary Fig. 4). Subsequently, cellular experimental analysis was performed to explore malignant biological behaviors of CATSPER1 in PAAD. CATSPER1 down-regulation was confirmed in Panc-1 and PATU-8988 cells through validation (Fig. 6G). Implementing the CCK-8 assay, Fig. 6H illustrated that the knockdown expression level of CATSPER1 significantly restrained the growth capacity of pancreatic cancer cells. CATSPER1 knockdown in pancreatic cancer cells resulted in a notable reduction in migrated cell numbers as demonstrated by the Transwell cell migration assay (Fig. 6I). Therefore, the down-regulated CATSPER1 expression inhibited the growth and migration abilities of pancreatic cancer cells, which corresponded with its pro-tumorigenic effect for patients with malignant pancreatic tumors.

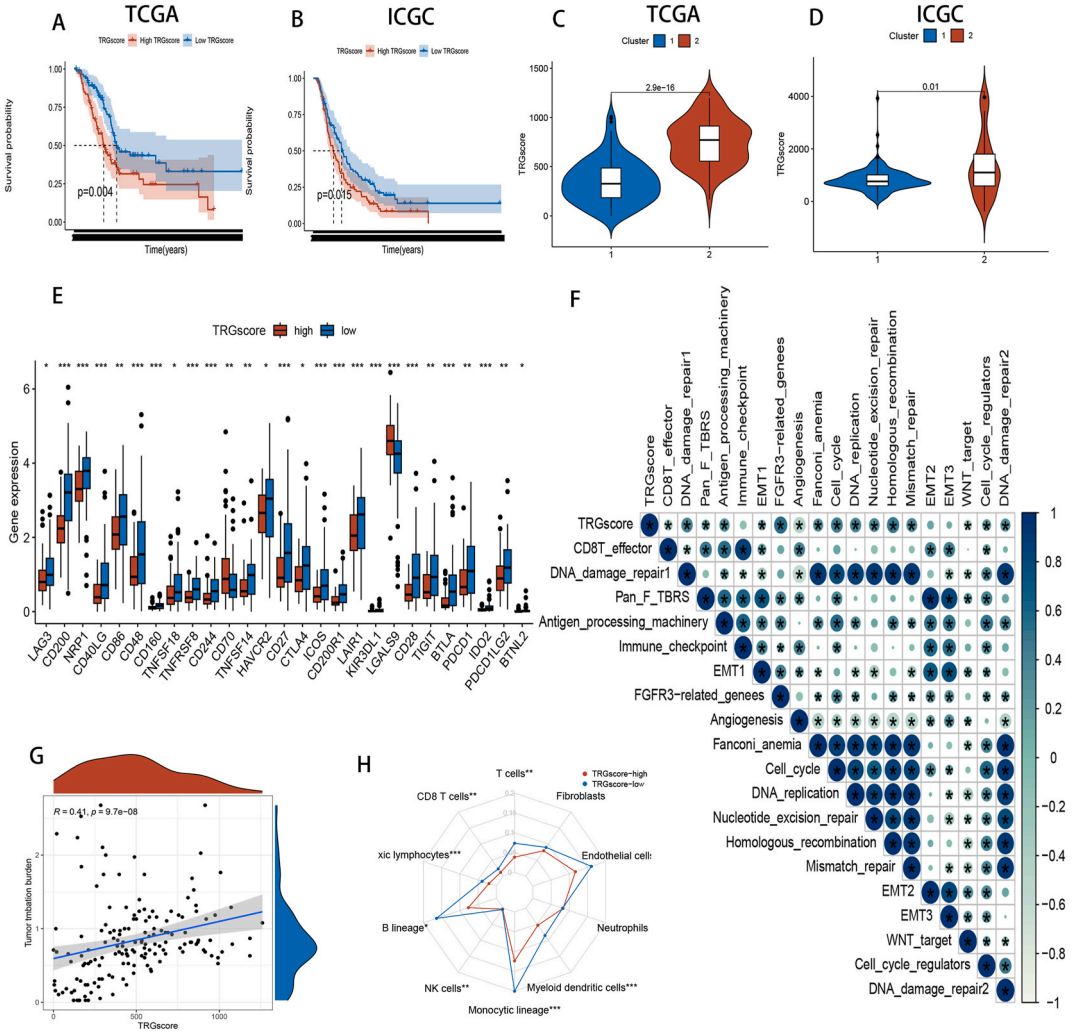

Fig. 7. Quantification of TTK related signatures based on TRGscore. Survival analysis was conducted for the overall survival (OS) in the TCGA-PAAD (A) and ICGC (B) cohorts, respectively. Correlations between the two TTK-relevant patterns and TRGscore in TCGA-PAAD (C) and ICGC (D) cohort, respectively. The TCGA-PAAD cohort(E) showed similar levels of immune checkpoint-related gene expression in both groups. Relationships between TRGscore and specific pathway patterns in the TCGA-PAAD cohort(F). Scatter plots show a strong positive correlation between TRGscore and TMB in the TCGA-PAAD cohort(G). MCPcounter(H) analyzed the variation in levels of immune cell infiltration between two groups in TCGA(H). *P < 0.05, **P < 0.01, ***P < 0.001, ****P < 0.0001.

3.7. TRGscore quantifies the TME in PAAD

TTK-related subgroups in individuals can be efficiently forecasted. Consequently, we applied PCA on the 41 DEGs and developed a scoring index defined as TRGscore to quantify the TTK-related status for each PAAD case (Supplementary Table 5). In the TCGA-PAAD cohort, the TRGscore-high pattern was associated with significantly worse survival compared to the TRGscore-low pattern (p-value = 0.004). Similarly, in the ICGC-PACA-CA cohort, the TRGscore-low pattern demonstrated a notable survival advantage (p-value = 0.015) (Fig. 7A and B). Additionally, comparing TRGscore levels among the TTK-related two patterns, TRGscore was higher in Cluster 2 than Cluster 1 (Wilcox test, P < 2.2e-16, Fig. 7C and D). A significant correlation was found between TRGscore and some clinico-pathological characteristics, such as stage and grade (Supplementary Fig. 5C). Additionally, the TRGscore may serve as a predictive factor through both univariate and multivariate Cox regression analyses (HR > 1; P < 0.005, Supplementary Figs. 5A–B). The TRGscore-low group is more abundant with expression of immune checkpoint inhibitors, implying that the samples in TRGscore-low subset are more inclined to benefit from ICB(Fig. 7E). Subsequently, a significant negative association was found between TRGscore and enrichment scores of $CD8^{+}$ T effectors in TCGA-PAAD and ICGC-PAAD-CA datasets by conducting the ssGSEA algorithm (Fig. 7F). Furthermore, we applied GSEA to further reveal the characteristics between high and low-TRGscore patterns according to KEGG (Supplementary Figs. 6A and B). Expectedly, gene sets were related to glycolysis, pentose phosphate pathway, and carcinogenic pathway enriched in the high-TRGscore group. These two metabolic pathways are correlated with poor outcomes in tumors [48,49]. On the contrary, we found enrichment in gene sets associated with immune activation in the low-TRGscore group. This consequence is consistent with our conclusion and validated by the ICGC-PAAD-CA cohort (Supplementary Fig. 7). Additionally, the TRGscore is positively correlated with TMB (Fig. 7G). The Phenomenon confirmed a more sensitive immunotherapy response in a low-TRGscore pattern.

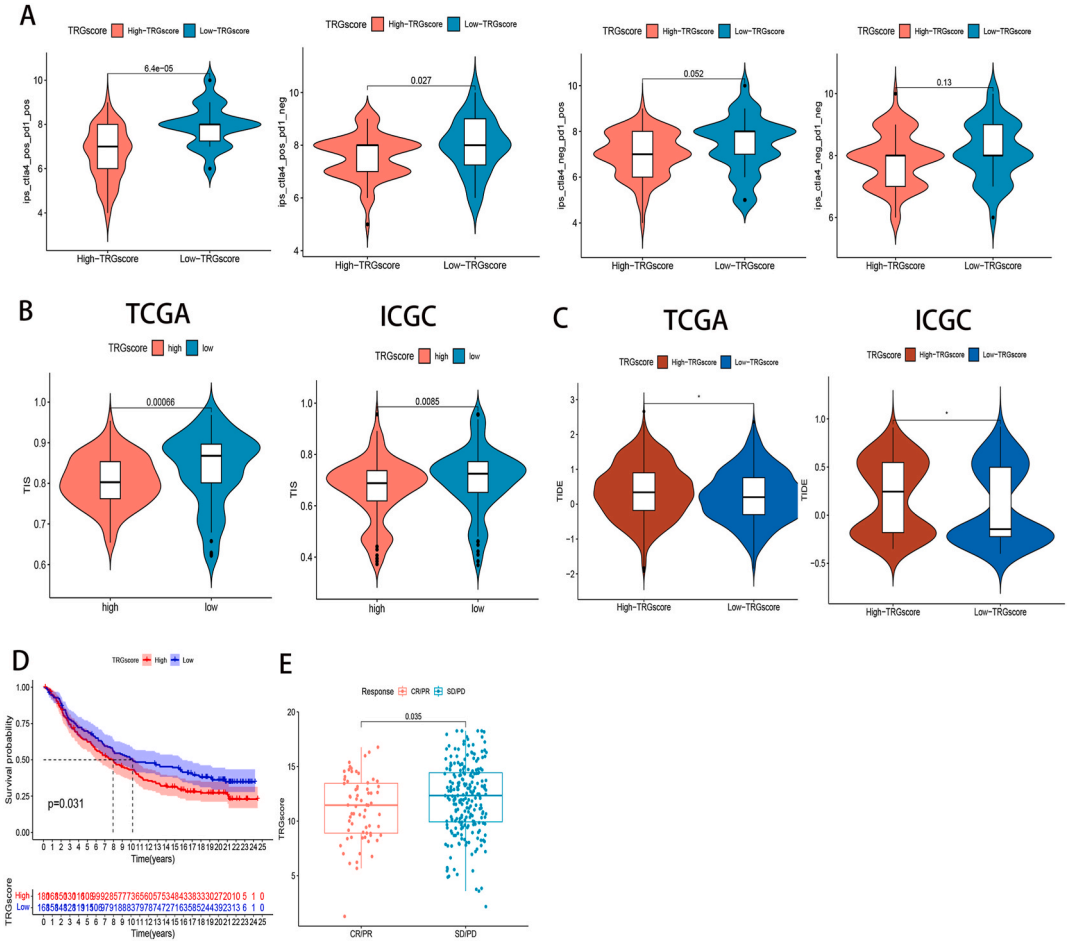

Fig. 8. TRGscore predicts the response of PAAD to Immunotherapy. Forecasting the response to immunotherapy (anti-PD-1 and anti-CTLA4) in the TRGscore high and low subgroups (A). TIS scores (B). TIDE score (C). The Kaplan–Meier curve based on high- and low- TRGscore groups in the IMvigor210 cohort (D). The Wilcoxon test was conducted to analyze the variation in TRGscore related to anti-PD-L1 responsiveness in the IMvigor210 cohort (E). *P < 0.05, **P < 0.01, ***P < 0.001, ****P < 0.0001.

3.8. Immune-related characteristics of TRGscore groups

The association between TRGscore groups and other defined subtypes was further explored to elaborately illustrate the heterogeneity of immunity between TRGscore groups. For immune subtypes defined by immune signatures, the low-TRGscore group exhibited a predominant C3-inflammatory subtype, while the high-TRGscore group exhibited dominant C1-wound healing and C2-IFN-gamma subtype (Supplementary Fig. 6C).

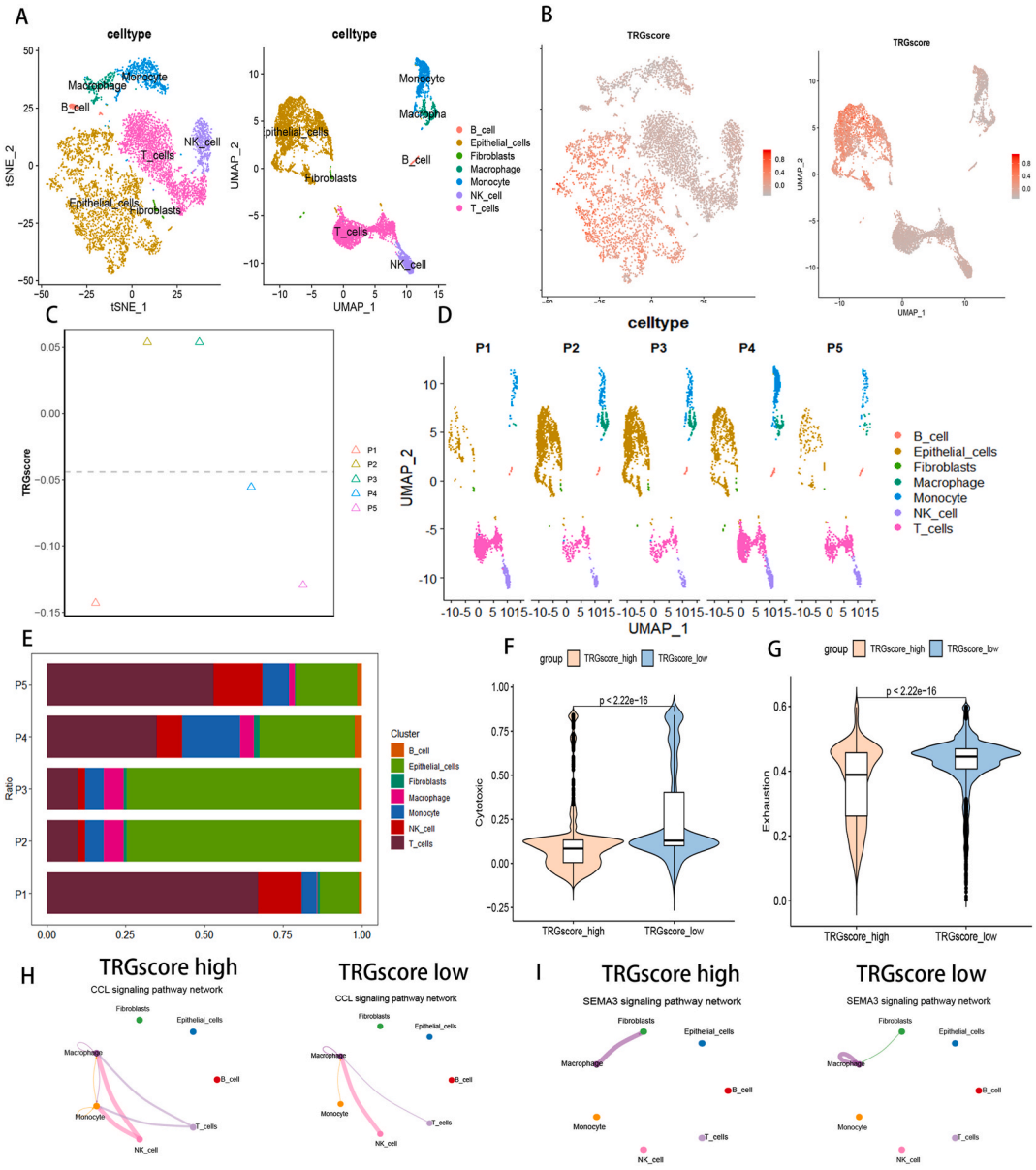

Fig. 9. ScRNA-seq analysis. Low TRGscore suggests an immune-active TME in the single cell cohort. t-SNE plot (left) and UMAP (right) plot showing the composition of 7 main subgroups derived from pancreatic cancer samples (A). The dynamics of TRGscore in 7 main cell types are showed in the t-SNE plot and UMAP plot (B).
Distribution in the TRGscore of five pancreatic cancer samples (separated into 2 patterns) (C). The distribution (D) and the proportion (E) of 7 main subtypes in five pancreatic cancer samples. Differences in cytotoxic score (F) and exhaustion (G) of T cells between two TRGscore related groups. Circos plots illustrating the CCL signaling pathways between high-TRGScore (left) and low-TRGScore (right) group (H). Circos plots illustrating the SEMA3 signaling pathways between high-TRGScore (left) and low-TRGScore (right) group (I).

3.9. The TRGscore determines the effectiveness of chemotherapy

Predictions were made and comparisons were drawn between the IC50 values of typical chemotherapy medications. Patients in the high-TRGscore pattern were more responsive to paclitaxel (P = 2.2e-7), erlotinib (P = 3.6e-6), and mitomycin C (P = 0.005). In contrast, patients in the low-TRGscore pattern were more susceptible to cisplatin (P = 0.00033) (Supplementary Fig. 6D).

3.10. TRGscore predicts the response of pancreatic cancer to immunotherapy

We furthermore explore whether TRGscore apply to predict immunotherapy sensibility in PAAD patients. Patients with low TRGscore had higher TIS and IPS compared to those with high TRGscore (Fig. 8A and B). Patients who have a high TIDE predictive score are fewer likely to gain benefit from immunotherapy because their immune system is more likely to escape. Notably, those with high TRGscores had significantly higher TIDE scores than those with low TRGscores (Fig. 8C). Additionally, patients with low TRGscores had better survival prognoses in the IMivgor210 cohort (Fig. 8D). Predictably, individuals diagnosed with urothelial carcinoma and possessing lower TRGscores exhibited a higher probability of reacting positively to anti-PD-L1 immunotherapy (Fig. 8E). These findings suggest that patients with a low TRGscore are more likely to benefit from immunotherapy.

3.11. scRNA dataset analysis

We further tried to explore crucial roles in the TME that contribute to TTK-related phenotypes. We extracted five primary tumors from single-cell mRNA profiles, GSE156405. All filter cells are divided into seven major types, containing B cells, epithelial cells, fibroblasts, macrophage, monocytes, NK cells, and T cells, under quality control and removal of batch effects (Fig. 9A and B). Five tumor samples were separated into high and low-TRGscore sets (Fig. 9C). Surprisingly, an obviously higher proportion of T cells and a fewer proportion of epithelial cells were found in low-TRGscore sets (Fig. 9D and E). Moreover, samples with low TRGscore have higher cytotoxic and exhaustion scores of the T cells (P = 2.2E-16) (Fig. 9F and G). Additionally, the glycolysis, hypoxia, and carcinogen pathways are enriched in the TRGscore-high subgroups. On the contrary, the immune and inflammatory pathways are enriched in the TRGscore-low subgroups (Supplementary Fig. 8A). This is consistent with a previous result.

3.12. Cell–cell communication in the high-TRGscore group could promote PAAD progression

Interactions between cells could have a significant impact on the high-TRGscore group beyond the internal cellular conditions. Additionally, we found that CCL [49,50], SEMA3 [51,52], and AREG-EGFR [53] signaling networks were strengthened in the high-TRGscore group, which was acknowledged as risk factors that can promote PAAD progression and inhibit immune microenvironment (Fig. 9H and I). Furthermore, we constructed an interactive map to explore the difference in intercellular communications of epithelial cells among two patterns, given that epithelial tumor cells take indispensable roles in the entire TME and the great extent of interactions between epithelial tumor cells and other cells contribute to tumorigenesis (Supplementary Fig. 8B). Enhanced communication from epithelial cells to neighboring cells was detected in the TRGscore-high profiles, including NAMPT-(ITGA5+ITGB1), MIF-($CD74^{+}$CD44), MIF-(CD74+CXCR4), ANGPTL4-SDC2, ANGPTL4-CDH11, and ANGPTL4-(ITGA5+ITGB1), which have the potential to promote tumor spread, growth, and evasion of the immune system [54–58]. In conclusion, these results favor the negative relationship between the TRGscore and favorable outcomes and immune activity.

3.13. Mapping malignancy-specific regulon networks by SCENIC

Next, we utilized SCENIC to explore TF motif activity in our scPAAD-seq data. Hierarchical clustering to distinguish TFs revealed the same and distinct regulatory elements across cell types (Supplementary Fig. 8C and Supplementary Table S6). The characteristic of different lineage-specific TFs further confirmed our identification of cell identities. For example, KLF5 has the ability to enhance tumor growth, transformation of acinar cells into ductal cells, and development of pancreatic intraepithelial neoplasia in PAAD [59]. HDAC2 facilitates the loss of primary cilia in PAAD [60]. ETS1 is highly expressed in T lymphocytes [61]. CEBPβ can promote the expression of CXCL8, TNFSF11, CSF3, and CCL2 by monocyte cell line [62].

4. Discussion

Immunotherapy is one of the important measures in multiple malignancies. But only a subset of patients with PAAD is sensitive to these therapies due to the complicated TME [63]. Therefore, identifying the heterogeneity of TME in PAAD and selecting the patient population who are suitable for immunotherapy is prominently significant. In the present study, combining multi-omics datasets and single-cell RNAseq feature the heterogeneity of PAAD at the inter- and intratumor angles via exploring the levels of multiple immune cells infiltrating among different patterns. We distinguish two different TTK-related subtypes of PAAD based on GSTTK identified by high-throughput experimental methods. Cluster 1, associated with a favorable prognosis, is more abundant with immune cells and has a better immune response. Cluster 2, correlated with poor outcomes, has a higher level of immunosuppressive signatures and more obvious genetic variation, containing mutational signatures, somatic mutations, and related signaling pathways.

Some studies indicated that the abnormity of CATSPER1 contributes to infertility [64,65]. The growth of colon cancer cells is regulated by CATSPER1 expression through the PI3K/AKT signaling pathway [66]. In this new research, it was discovered for the first

time that CATSPER1 has increased levels in pancreatic cancer cells compared to normal tissue, and through experimentation, it was found to promote the proliferation and migration of PAAD cells.

Moreover, we constructed a scoring system named the TRGscore, and multi-bulk RNA and single-cell datasets could be precisely classified utilizing the TRGscore. A high TRGscore was significantly associated with high TMB and poor clinical outcomes, while a low TRGscore was correlated with abundant immune cell infiltration. Additionally, our study indicated an immunosuppression-specific TF regulation and interaction network in the TME cells of the high-TRGscore subgroup.

There was a direct relationship discovered between the extent of immune cell penetration and the effectiveness of immunotherapy. Several research studies suggested that blocking PD-L1 could successfully inhibit pancreatic adenocarcinoma in a mouse model by increasing IFN-g levels and reducing IL-10 production [67]. Moreover, PD-L1-positive tumors exhibit a higher presence of tumor-infiltrating Tregs compared to negative tumors [67]. The results justified the use of therapy aimed at the PD-1/PD-L1 pathway for treating pancreatic cancer. The features and positioning of immune cells within the TME, along with their response to immunotherapy, are now recognized as a predictive factor [68]. The current study acquired an enriched immune infiltration pattern (Cluster 1), defined as a "hot tumor," and another "cold tumor" (Cluster 2). Furthermore, we learned the "hot tumor" subtype, which had a finer outcome with abundant contents of cytotoxic genes, such as GZMA and PRF1, and T-cell activation genes, such as ZAP70, ITK, and IL2RB. These two distinguishing immune patterns have also existed in single-cell datasets. These analyses illustrated that patients with different immune features trigger different survival outcomes. Interestingly, the subtypes classified as 'cold tumors' exhibited elevated TMB levels, potentially resulting in immunosuppression and resistance to PD-L1/PD-1 blockade as standalone treatments [43,69]. Additionally, the TRGscore is negatively correlated with CD8 effector activity and positively associated with TMB (Fig. 7F and G). TMPRSS4, GPRC5a, and LINC01133 are three of the most score coefficient genes in the TRGscore. TMPRSS4 facilitates cell development by stimulating the ERK1/2 signaling pathway in PAAD [70]. GPRC5a promotes cell proliferation and migration in PAAD and leads to resistance to the common chemotherapy drug [71]. Knockout of LINC01133 reduced PAAD proliferation by activating the Wnt signaling pathway [72]. PAAD is resistant to single immunotherapy [73,74], attributed to inherent intratumor heterogeneity and immunosuppressive TME [75–77]. Combining immunotherapy and chemotherapy has proved to have better therapeutic effects in patients with PAAD. A recent study showed that combining PD-1 antagonist with gemcitabine led to improve survival compared with gemcitabine alone in a PAAD mouse model. Moreover, the content of CD8 T cells was increased in the combination therapy cohort [78].

The TRGscore was greatly accurate in predicting patient survival. The poor results of the elevated TRGscore group could be due to the activation of anti-immune factors that promote tumor immune evasion. Moreover, TRGscore showed a negative correlation with the extent of immune cell infiltration in pancreatic adenocarcinoma. We validated these findings in single cell sequencing level. The effectiveness of immunotherapy response was investigated using TIDE and TIS scores; individuals with low TRGscores, elevated TIDE scores, and increased TIS scores showed improved response, potentially due to reduced tumor immune evasion through T cell exclusion. Notably, in the IMivgor210 cohort, the low TRGscore group responded better. We can rely on the TRGscore to determine their suitability for immunotherapy and select appropriate chemotherapy drugs for patients. In general, the findings indicate that TRGscore has the potential to be a valuable resource for developing improved PAAD treatment strategies.

Naturally, there were also certain constraints in our study. Since we obtained our study groups from various high-throughput sequencing platforms across multiple publicly accessible datasets, it was inevitable to encounter intrapatient or intratumor tumor heterogeneity. Depending on the tumor heterogeneity, immunotherapy or chemotherapy may have different effects. So large-scale prospective studies are needed. Furthermore, we have not fully explored the functions of CATSPER1 in PAAD through experiments. Therefore, the underlying mechanisms of the CATSPER1 in PAAD should be conducted in the future.

5. Conclusions

Two distinct TTK patterns were identified using GSTTK, offering a glimpse into T cell function in PAAD. Moreover, we revealed the underlying heterogeneity among the two TTK patterns that contain immune characteristics, such as the sensitivity of ICB and multi-omics properties. Furthermore, for the first time, we found that CATSPER1 has a higher expression in pancreatic cancer cells than in normal tissue experiments and can stimulate PAAD cell proliferation and migration. In the end, we developed the TRGscore, which was confirmed using both bulk and single-cell transcriptome data, serving as a standalone predictor for PAAD. This offers a strong indicator for the prognosis and treatment response of PAAD patients. We will collect large-scale clinical validation samples and further conduct experiments to validate our results in the future.

Data availability statement

The original contributions presented in the study are included in the article/Supplementary Material, further inquiries can be directed to the corresponding authors. Data associated with this study has been deposited at The datasets used and/or analyzed during the current study are available in the Genotype Tissue Expression Project (GTEx) (https://www.gtexportal.org/), Gene Expression Omnibus (GEO, https://www.ncbi.nlm.nih.gov/geo/), The Cancer Genome Atlas (TCGA) network (https://cancergenome.nih.gov/) and International Cancer Genome Consortium (ICGC, https://dcc.icgc.org/). R and other custom scripts for analyzing data are available upon reasonable request.

Ethics statement

This study was reviewed and approved by the Ethics Committee of the First Affiliated Hospital of Wenzhou Medical University [ys 2022 (043)] in June 2020. The patients/participants provided their written informed consent to participate in this study. The questionnaires were anonymized, and patients were free to opt out of participation in the study whenever they were uncomfortable.

CRediT authorship contribution statement

Yin-wei Dai: Conceptualization. **Ya-ting Pan:** Formal analysis, Data curation. **Dan-feng Lin:** Methodology, Investigation. **Xiao-hu Chen:** Visualization, Validation, Software. **Xiang Zhou:** Writing – review & editing, Writing – original draft. **Wei-ming Wang:** Writing – review & editing, Writing – original draft, Resources, Funding acquisition.

Declaration of competing interest

The authors declare that they have no known competing financial interests or personal relationships that could have appeared to influence the work reported in this paper.

Acknowledgements

This study was supported by the funding of the Zhejiang Provincial Natural Science Foundation of China under grant(No. LQ20H160015) and the Wenzhou Medical University Research expenses project (KYYW202125).

Appendix A. Supplementary data

Supplementary data to this article can be found online at https://doi.org/10.1016/j.heliyon.2024.e27216.

References

[1] R. Goess, H. Friess, A look at the progress of treating pancreatic cancer over the past 20 years, Expet Rev. Anticancer Ther. 18 (3) (2018) 295–304.
[2] K.E. Caldwell, C.W. Hammill, Screening for pancreatic ductal adenocarcinoma: are we asking the impossible?-response, Cancer Prev. Res. 14 (10) (2021) 975–976. Philadelphia, Pa.
[3] J.P. Neoptolemos, J. Kleeff, P. Michl, E. Costello, W. Greenhalf, D.H. Palmer, Therapeutic developments in pancreatic cancer: current and future perspectives, Nat. Rev. Gastroenterol. Hepatol. 15 (6) (2018) 333–348.
[4] M.T. Roth, D.B. Cardin, J.D. Berlin, Recent advances in the treatment of pancreatic cancer, F1000Research 9 (2020).
[5] Y. Sunami, J. Kleeff, Immunotherapy of pancreatic cancer, Prog. Molec. Biol. Transl. Sci. 164 (2019) 189–216.
[6] W.F. Hong, M.Y. Liu, L. Liang, Y. Zhang, Z.J. Li, K. Han, S.S. Du, Y.J. Chen, L.H. Ma, Molecular characteristics of T cell-mediated tumor killing in hepatocellular carcinoma, Front. Immunol. 13 (2022) 868480.
[7] C. Zhang, J. Ding, X. Xu, Y. Liu, W. Huang, L. Da, Q. Ma, S. Chen, Tumor microenvironment characteristics of pancreatic cancer to determine prognosis and immune-related gene signatures, Front. Mol. Biosci. 8 (2021) 645024.
[8] D. Xu, Y. Wang, Y. Chen, J. Zheng, Identification of the molecular subtype and prognostic characteristics of pancreatic cancer based on CD8 + T cell-related genes, Cancer Immunol. Immunother. 72 (3) (2023) 647–664. CII.
[9] D. Pan, A. Kobayashi, P. Jiang, L. Ferrari de Andrade, R.E. Tay, A.M. Luoma, D. Tsoucas, X. Qiu, K. Lim, P. Rao, et al., A major chromatin regulator determines resistance of tumor cells to T cell-mediated killing, Science (New York, N.Y.) 359 (6377) (2018) 770–775.
[10] B. Ru, C.N. Wong, Y. Tong, J.Y. Zhong, S.S.W. Zhong, W.C. Wu, K.C. Chu, C.Y. Wong, C.Y. Lau, I. Chen, et al., TISIDB: an integrated repository portal for tumor-immune system interactions, Bioinformatics 35 (20) (2019) 4200–4202.
[11] C. Hutter, J.C. Zenklusen, The cancer genome Atlas: creating lasting value beyond its data, Cell 173 (2) (2018) 283–285.
[12] J. Zhang, R. Bajari, D. Andric, F. Gerthoffert, A. Lepsa, H. Nahal-Bose, L.D. Stein, V. Ferretti, The international cancer genome Consortium data portal, Nat. Biotechnol. 37 (4) (2019) 367–369.
[13] E. Clough, T. Barrett, The gene expression Omnibus database, Methods Mol. Biol. 1418 (2016) 93–110.
[14] A.M. Newman, C.L. Liu, M.R. Green, A.J. Gentles, W. Feng, Y. Xu, C.D. Hoang, M. Diehn, A.A. Alizadeh, Robust enumeration of cell subsets from tissue expression profiles, Nat. Methods 12 (5) (2015) 453–457.
[15] E. Becht, N.A. Giraldo, L. Lacroix, B. Buttard, N. Elarouci, F. Petitprez, J. Selves, P. Laurent-Puig, C. Sautès-Fridman, W.H. Fridman, et al., Estimating the population abundance of tissue-infiltrating immune and stromal cell populations using gene expression, Genome Biol. 17 (1) (2016) 218.
[16] H. Hackl, P. Charoentong, F. Finotello, Z. Trajanoski, Computational genomics tools for dissecting tumour-immune cell interactions, Nat. Rev. Genet. 17 (8) (2016) 441–458.
[17] D.S. Chen, I. Mellman, Oncology meets immunology: the cancer-immunity cycle, Immunity 39 (1) (2013) 1–10.
[18] K. Yoshihara, M. Shahmoradgoli, E. Martínez, R. Vegesna, H. Kim, W. Torres-Garcia, V. Treviño, H. Shen, P.W. Laird, D.A. Levine, et al., Inferring tumour purity and stromal and immune cell admixture from expression data, Nat. Commun. 4 (2013) 2612.
[19] S. Mariathasan, S.J. Turley, D. Nickles, A. Castiglioni, K. Yuen, Y. Wang, E.E. Kadel III, H. Koeppen, J.L. Astarita, R. Cubas, et al., TGFβ attenuates tumour response to PD-L1 blockade by contributing to exclusion of T cells, Nature 554 (7693) (2018) 544–548.
[20] J.E. Rosenberg, J. Hoffman-Censits, T. Powles, M.S. van der Heijden, A.V. Balar, A. Necchi, N. Dawson, P.H. O'Donnell, A. Balmanoukian, Y. Loriot, et al., Atezolizumab in patients with locally advanced and metastatic urothelial carcinoma who have progressed following treatment with platinum-based chemotherapy: a single-arm, multicentre, phase 2 trial, Lancet (London, England) 387 (10031) (2016) 1909–1920.
[21] Y. Şenbabaoğlu, R.S. Gejman, A.G. Winer, M. Liu, E.M. Van Allen, G. de Velasco, D. Miao, I. Ostrovnaya, E. Drill, A. Luna, et al., Tumor immune microenvironment characterization in clear cell renal cell carcinoma identifies prognostic and immunotherapeutically relevant messenger RNA signatures, Genome Biol. 17 (1) (2016) 231.
[22] P. Charoentong, F. Finotello, M. Angelova, C. Mayer, M. Efremova, D. Rieder, H. Hackl, Z. Trajanoski, Pan-cancer immunogenomic analyses reveal genotype-immunophenotype relationships and predictors of response to checkpoint blockade, Cell Rep. 18 (1) (2017) 248–262.

[23] N. Auslander, G. Zhang, J.S. Lee, D.T. Frederick, B. Miao, T. Moll, T. Tian, Z. Wei, S. Madan, R.J. Sullivan, et al., Robust prediction of response to immune checkpoint blockade therapy in metastatic melanoma, Nat. Med. 24 (10) (2018) 1545–1549.
[24] P.L. Chen, W. Roh, A. Reuben, Z.A. Cooper, C.N. Spencer, P.A. Prieto, J.P. Miller, R.L. Bassett, V. Gopalakrishnan, K. Wani, et al., Analysis of immune signatures in longitudinal tumor samples yields insight into biomarkers of response and mechanisms of resistance to immune checkpoint blockade, Cancer Discov. 6 (8) (2016) 827–837.
[25] M. Ayers, J. Lunceford, M. Nebozhyn, E. Murphy, A. Loboda, D.R. Kaufman, A. Albright, J.D. Cheng, S.P. Kang, V. Shankaran, et al., IFN-γ-related mRNA profile predicts clinical response to PD-1 blockade, J. Clin. Invest. 127 (8) (2017) 2930–2940.
[26] Q. Zhang, Y. Tan, J. Zhang, Y. Shi, J. Qi, D. Zou, W. Ci, Pyroptosis-related signature predicts prognosis and immunotherapy efficacy in muscle-invasive bladder cancer, Front. Immunol. 13 (2022) 782982.
[27] B. Zhang, Q. Wu, B. Li, D. Wang, L. Wang, Y.L. Zhou, m(6)A regulator-mediated methylation modification patterns and tumor microenvironment infiltration characterization in gastric cancer, Mol. Cancer 19 (1) (2020) 53.
[28] A. Butler, P. Hoffman, P. Smibert, E. Papalexi, R. Satija, Integrating single-cell transcriptomic data across different conditions, technologies, and species, Nat. Biotechnol. 36 (5) (2018) 411–420.
[29] C. Liang, Y. Qin, B. Zhang, S. Ji, S. Shi, W. Xu, J. Liu, J. Xiang, D. Liang, Q. Hu, et al., ARF6, induced by mutant Kras, promotes proliferation and Warburg effect in pancreatic cancer, Cancer Lett. 388 (2017) 303–311.
[30] Y. Jing, W. Liang, J. Liu, L. Zhang, J. Wei, Y. Zhu, J. Yang, K. Ji, Y. Zhang, Z. Huang, Stress-induced phosphoprotein 1 promotes pancreatic cancer progression through activation of the FAK/AKT/MMP signaling axis, Pathol. Res. Pract. 215 (11) (2019) 152564.
[31] S. Slovin, A. Carissimo, F. Panariello, A. Grimaldi, V. Bouché, G. Gambardella, D. Cacchiarelli, Single-cell RNA sequencing analysis: a step-by-step Overview, Methods Mol. Biol. 2284 (2021) 343–365.
[32] S. Jin, C.F. Guerrero-Juarez, L. Zhang, I. Chang, R. Ramos, C.H. Kuan, P. Myung, M.V. Plikus, Q. Nie, Inference and analysis of cell-cell communication using CellChat, Nat. Commun. 12 (1) (2021) 1088.
[33] S. Aibar, C.B. González-Blas, T. Moerman, V.A. Huynh-Thu, H. Imrichova, G. Hulselmans, F. Rambow, J.C. Marine, P. Geurts, J. Aerts, et al., SCENIC: single-cell regulatory network inference and clustering, Nat. Methods 14 (11) (2017) 1083–1086.
[34] J.M. Kim, D.S. Chen, Immune escape to PD-L1/PD-1 blockade: seven steps to success (or failure), Ann. Oncol.: Off. J. Eur. Soc. Med. Oncol. 27 (8) (2016) 1492–1504.
[35] A. Kallies, D. Zehn, D.T. Utzschneider, Precursor exhausted T cells: key to successful immunotherapy? Nat. Rev. Immunol. 20 (2) (2020) 128–136.
[36] M. Yi, X. Zheng, M. Niu, S. Zhu, H. Ge, K. Wu, Combination strategies with PD-1/PD-L1 blockade: current advances and future directions, Mol. Cancer 21 (1) (2022) 28.
[37] Y. Tabana, T.C. Moon, A. Siraki, S. Elahi, K. Barakat, Reversing T-cell exhaustion in immunotherapy: a review on current approaches and limitations, Expert Opin. Ther. Targets 25 (5) (2021) 347–363.
[38] M. Hashimoto, A.O. Kamphorst, S.J. Im, H.T. Kissick, R.N. Pillai, S.S. Ramalingam, K. Araki, R. Ahmed, CD8 T cell exhaustion in chronic infection and cancer: opportunities for interventions, Annu. Rev. Med. 69 (2018) 301–318.
[39] X. Chen, H. Chen, H. Yao, K. Zhao, Y. Zhang, D. He, Y. Zhu, Y. Cheng, R. Liu, R. Xu, et al., Turning up the heat on non-immunoreactive tumors: pyroptosis influences the tumor immune microenvironment in bladder cancer, Oncogene 40 (45) (2021) 6381–6393.
[40] Y. Xiao, D. Ma, S. Zhao, C. Suo, J. Shi, M.Z. Xue, M. Ruan, H. Wang, J. Zhao, Q. Li, et al., Multi-omics profiling reveals distinct microenvironment characterization and suggests immune escape mechanisms of triple-negative breast cancer, Clin. Cancer Res.: Off. J. Am. Assoc. Cancer Res. 25 (16) (2019) 5002–5014.
[41] C. Curcio, S. Brugiapaglia, S. Bulfamante, L. Follia, P. Cappello, F. Novelli, The glycolytic pathway as a target for novel onco-immunology therapies in pancreatic cancer, Molecules 26 (6) (2021).
[42] M.D. Wellenstein, K.E. de Visser, Cancer-cell-intrinsic mechanisms shaping the tumor immune landscape, Immunity 48 (3) (2018) 399–416.
[43] Y. Pico de Coaña, A. Choudhury, R. Kiessling, Checkpoint blockade for cancer therapy: revitalizing a suppressed immune system, Trends Mol. Med. 21 (8) (2015) 482–491.
[44] M. Gu, Y. Gao, P. Chang, KRAS mutation dictates the cancer immune environment in pancreatic ductal adenocarcinoma and other adenocarcinomas, Cancers 13 (10) (2021).
[45] Y. Cui, G. Guo, Immunomodulatory function of the tumor suppressor p53 in host immune response and the tumor microenvironment, Int. J. Mol. Sci. 17 (11) (2016).
[46] J.A. McCubrey, L.V. Yang, S.L. Abrams, L.S. Steelman, M.Y. Follo, L. Cocco, S. Ratti, A.M. Martelli, G. Augello, M. Cervello, Effects of TP53 mutations and miRs on immune responses in the tumor microenvironment important in pancreatic cancer progression, Cells 11 (14) (2022).
[47] Y. Qian, Y. Gong, Z. Fan, G. Luo, Q. Huang, S. Deng, H. Cheng, K. Jin, Q. Ni, X. Yu, et al., Molecular alterations and targeted therapy in pancreatic ductal adenocarcinoma, J. Hematol. Oncol. 13 (1) (2020) 130.
[48] T.J. Yu, D. Ma, Y.Y. Liu, Y. Xiao, Y. Gong, Y.Z. Jiang, Z.M. Shao, X. Hu, G.H. Di, Bulk and single-cell transcriptome profiling reveal the metabolic heterogeneity in human breast cancers, Mol. Ther.: J. Am. Soc. Gene Therapy 29 (7) (2021) 2350–2365.
[49] Y.W. Dai, H.B. Chen, Y.T. Pan, L.X. Lv, W.M. Wang, X.H. Chen, X. Zhou, Characterization of chromatin regulators identified prognosis and heterogeneity in hepatocellular carcinoma, Front. Oncol. 12 (2022) 1002781.
[50] H. Gu, W. Deng, Z. Zheng, K. Wu, F. Sun, CCL2 produced by pancreatic ductal adenocarcinoma is essential for the accumulation and activation of monocytic myeloid-derived suppressor cells, Immun. Inflamm. Disease 9 (4) (2021) 1686–1695.
[51] D. Zhang, A. Lindstrom, E.J. Kim, C.I. Hwang, M.L. Hall, T.Y. Lin, Y. Li, SEMA3C supports pancreatic cancer progression by regulating the autophagy process and tumor immune microenvironment, Front. Oncol. 12 (2022) 890154.
[52] X. Zhang, B. Klamer, J. Li, S. Fernandez, L. Li, A pan-cancer study of class-3 semaphorins as therapeutic targets in cancer, BMC Med. Genom. 13 (Suppl 5) (2020) 45.
[53] L. Wang, L. Wang, H. Zhang, J. Lu, Z. Zhang, H. Wu, Z. Liang, AREG mediates the epithelial-mesenchymal transition in pancreatic cancer cells via the EGFR/ERK/NF-κB signalling pathway, Oncol. Rep. 43 (5) (2020) 1558–1568.
[54] H.Q. Ju, Z.N. Zhuang, H. Li, T. Tian, Y.X. Lu, X.Q. Fan, H.J. Zhou, H.Y. Mo, H. Sheng, P.J. Chiao, et al., Regulation of the Nampt-mediated NAD salvage pathway and its therapeutic implications in pancreatic cancer, Cancer Lett. 379 (1) (2016) 1–11.
[55] T. Zhu, R. Chen, J. Wang, H. Yue, X. Lu, J. Li, The prognostic value of ITGA and ITGB superfamily members in patients with high grade serous ovarian cancer, Cancer Cell Int. 20 (2020) 257.
[56] L. Yang, R. Sun, Y. Wang, Y. Fu, Y. Zhang, Z. Zheng, Z. Ji, D. Zhao, Expression of ANGPTL2 and its impact on papillary thyroid cancer, Cancer Cell Int. 19 (2019) 204.
[57] S.H. Kim, Y.Y. Park, S.W. Kim, J.S. Lee, D. Wang, R.N. DuBois, ANGPTL4 induction by prostaglandin E2 under hypoxic conditions promotes colorectal cancer progression, Cancer Res. 71 (22) (2011) 7010–7020.
[58] K. Liu, Y. Geng, L. Wang, H. Xu, M. Zou, Y. Li, Z. Zhao, T. Chen, F. Xu, L. Sun, et al., Systematic exploration of the underlying mechanism of gemcitabine resistance in pancreatic adenocarcinoma, Mol. Oncol. 16 (16) (2022) 3034–3051.
[59] P. He, J.W. Yang, V.W. Yang, A.B. Bialkowska, Krüppel-like factor 5, increased in pancreatic ductal adenocarcinoma, promotes proliferation, acinar-to-ductal metaplasia, pancreatic intraepithelial neoplasia, and tumor growth in mice, Gastroenterology 154 (5) (2018) 1494–1508.e1413.
[60] T. Kobayashi, K. Nakazono, M. Tokuda, Y. Mashima, B.D. Dynlacht, H. Itoh, HDAC2 promotes loss of primary cilia in pancreatic ductal adenocarcinoma, EMBO Rep. 18 (2) (2017) 334–343.
[61] M. Testoni, E.Y. Chung, V. Priebe, F. Bertoni, The transcription factor ETS1 in lymphomas: friend or foe? Leuk. Lymphoma 56 (7) (2015) 1975–1980.
[62] J. Ma, X. Yang, X. Chen, C/EBPβ is a key transcription factor of ox-LDL inducing THP-1 cells to release multiple pro-inflammatory cytokines, Inflamm. Res.: Off. J. Eur. Histamine Res. Soc. [et al] 70 (10-12) (2021) 1191–1199.

[63] A.H. Morrison, K.T. Byrne, R.H. Vonderheide, Immunotherapy and prevention of pancreatic cancer, Trends Cancer 4 (6) (2018) 418–428.
[64] M.R. Avenarius, M.S. Hildebrand, Y. Zhang, N.C. Meyer, L.L. Smith, K. Kahrizi, H. Najmabadi, R.J. Smith, Human male infertility caused by mutations in the CATSPER1 channel protein, Am. J. Hum. Genet. 84 (4) (2009) 505–510.
[65] A.E. Carlson, R.E. Westenbroek, T. Quill, D. Ren, D.E. Clapham, B. Hille, D.L. Garbers, D.F. Babcock, CatSper1 required for evoked Ca2+ entry and control of flagellar function in sperm, Proc. Natl. Acad. Sci. U.S.A. 100 (25) (2003) 14864–14868.
[66] Y. Huang, Y. Wang, Z. Wu, T. Li, S. Li, C. Wang, J. Ao, C. Yang, Y. Zhou, SOX11-dependent CATSPER1 expression controls colon cancer cell growth through regulation the PI3K/AKT signaling pathway, Genes Genom. 44 (11) (2022) 1415–1424.
[67] M. Loos, N.A. Giese, J. Kleeff, T. Giese, M.M. Gaida, F. Bergmann, M. Laschinger, M.W. Büchler, H. Friess, Clinical significance and regulation of the costimulatory molecule B7-H1 in pancreatic cancer, Cancer Lett. 268 (1) (2008) 98–109.
[68] J.S. O'Donnell, M.W.L. Teng, M.J. Smyth, Cancer immunoediting and resistance to T cell-based immunotherapy, Nat. Rev. Clin. Oncol. 16 (3) (2019) 151–167.
[69] M. Feng, G. Xiong, Z. Cao, G. Yang, S. Zheng, X. Song, L. You, L. Zheng, T. Zhang, Y. Zhao, PD-1/PD-L1 and immunotherapy for pancreatic cancer, Cancer Lett. 407 (2017) 57–65.
[70] J. Gu, W. Huang, J. Zhang, X. Wang, T. Tao, L. Yang, Y. Zheng, S. Liu, J. Yang, L. Zhu, et al., TMPRSS4 promotes cell proliferation and inhibits apoptosis in pancreatic ductal adenocarcinoma by activating ERK1/2 signaling pathway, Front. Oncol. 11 (2021) 628353.
[71] B. Liu, H. Yang, C. Pilarsky, G.F. Weber, The effect of GPRC5a on the proliferation, migration ability, chemotherapy resistance, and phosphorylation of GSK-3β in pancreatic cancer, Int. J. Mol. Sci. 19 (7) (2018).
[72] Y.C. Weng, J. Ma, J. Zhang, J.C. Wang, Long non-coding RNA LINC01133 silencing exerts antioncogenic effect in pancreatic cancer through the methylation of DKK1 promoter and the activation of Wnt signaling pathway, Cancer Biol. Ther. 20 (3) (2019) 368–380.
[73] J.R. Brahmer, S.S. Tykodi, L.Q. Chow, W.J. Hwu, S.L. Topalian, P. Hwu, C.G. Drake, L.H. Camacho, J. Kauh, K. Odunsi, et al., Safety and activity of anti-PD-L1 antibody in patients with advanced cancer, N. Engl. J. Med. 366 (26) (2012) 2455–2465.
[74] J. Kleeff, M. Korc, M. Apte, C. La Vecchia, C.D. Johnson, A.V. Biankin, R.E. Neale, M. Tempero, D.A. Tuveson, R.H. Hruban, et al., Pancreatic cancer, Nat. Rev. Dis. Prim. 2 (2016) 16022.
[75] M. Binnewies, E.W. Roberts, K. Kersten, V. Chan, D.F. Fearon, M. Merad, L.M. Coussens, D.I. Gabrilovich, S. Ostrand-Rosenberg, C.C. Hedrick, et al., Understanding the tumor immune microenvironment (TIME) for effective therapy, Nat. Med. 24 (5) (2018) 541–550.
[76] W.J. Ho, E.M. Jaffee, L. Zheng, The tumour microenvironment in pancreatic cancer - clinical challenges and opportunities, Nat. Rev. Clin. Oncol. 17 (9) (2020) 527–540.
[77] N. McGranahan, C. Swanton, Clonal heterogeneity and tumor evolution: past, present, and the future, Cell 168 (4) (2017) 613–628.
[78] J. Brooks, B. Fleischmann-Mundt, N. Woller, J. Niemann, S. Ribback, K. Peters, I.E. Demir, N. Armbrecht, G.O. Ceyhan, M.P. Manns, et al., Perioperative, spatiotemporally coordinated activation of T and NK cells prevents recurrence of pancreatic cancer, Cancer Res. 78 (2) (2018) 475–488.